ACS APPLIED MATERIALS & INTERFACES

Research Article

www.acsami.org

Simple Technique for Spatially Separated Nanofibers/Nanobeads by Multinozzle Electrospinning toward White-Light Emission

Jongho Kim, Jaeguk Noh, Seonyoung Jo, Ko Eun Park, Won Ho Park, and Taek Seung Lee*

Organic and Optoelectronic Materials Laboratory, Department of Advanced Organic Materials and Textile System Engineering, Chungnam National University, Daejeon 306-764, Korea

Supporting Information

ABSTRACT: Electrospun, emission color-tunable nanofibrous sheets were fabricated by multinozzle electrospinning equipped with a secondary electrode for the preparation of white-emissive sheets under a single excitation source, manipulating energy transfer between dyes. By control of the concentration of commercially available red, green, and blue dyes in the matrix polymer [poly(methyl methacrylate)], emission color tuning can be easily accomplished because each dye is located in spatially separated fibers to maintain enough distance to prevent or suppress energy transfer, allowing white-light emission. The application of dye separation for the white-light emission upon excitation with a blue light-emitting-diode lamp is demonstrated, indicative of its potential application for the easy and facile tuning of fluorescence color toward flexible illumination.

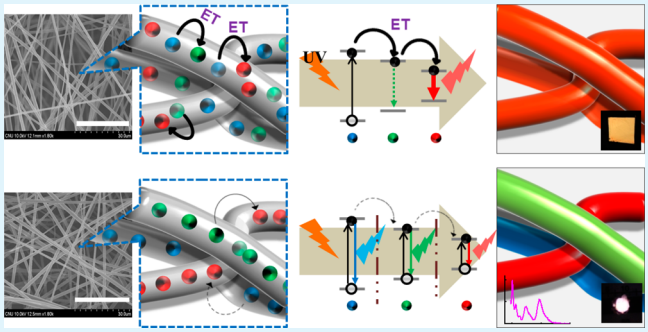

KEYWORDS: *electrospinning, nanofibers, white-light emission, fluorescence, multinozzle equipment*

INTRODUCTION

White-light-emitting devices based on organic molecules have received a great deal of attention in the fields of optoelectronics.[1−7] Because a broad emission spectrum is the essential requirement for white emission, it is not easy to obtain white emission using a single dye molecule.[8,9]

Practically, white-light emission can be achieved using a mixture of three primary dyes, emitting red (R), green (G), and blue (B) lights.[10,11] Mixing multiple emissive materials, unfortunately, results in emissive dyes being sufficiently close in proximity to interact with each other, thus leading to undesirable energy transfer (ET) from the dye with short-wavelength emission (donor B or G) to the dye with long-wavelength emission (acceptor G or R), which is an obstacle to obtaining a broad band of emission within the visible spectrum.[12,13]

Isolation of each emissive dye is highly recommended to solve this ET problem, using matrix materials to maintain minimal distance in which the interactions between donor and acceptor dyes become negligible. It has been reported that to attain efficient dye isolation, polymerization of inorganic compounds into thin films containing monomeric or polymeric dyes,[14,15] micelle formation in the polymer matrix,[16,17] and formation of protein luminescent films[18] have been carried out as controllable host−guest systems.[19,20]

Electrospinning is a technique that utilizes electrostatic force alone to fabricate nanofibers on a large scale.[21−29] Unlike conventional spinning techniques (solution and melt spinning), which are capable of manufacturing fibers with diameters in the micrometer range (ca. 5−25 μm), electrospinning is able to fabricate nanofibers with a much smaller diameter range of 10−1000 nm. The incorporation of optoelectronically active materials, such as conjugated polymers, quantum dots, and small molecules, into electrospun nanofibers is an attractive method to investigate their optical and electronic properties and to manufacture optoelectronic devices on the nanometer scale.[30−36]

Electrospun nanofibers with optoelectronic activities are generally prepared by spinning with an inert polymer such as polyimide or poly(ethylene oxide) (PEO), which serves as a supporting matrix.[37−39] Recently, light-emitting electrospun nanofibers with matrix polymers of PEO or polystyrene containing small dye molecules and conjugated polymers in the nanoscale dimension have been reported to emit light.[37,40,41] Moreover, electrospinning has emerged as a simple and low-cost method for the fabrication of nanoporous polymer composites, which have potential applications in enhanced sensory systems.[23,42−45]

Electrospinning with low concentrations of matrix polymer enables the fabrication of particle-shaped products rather than fiber-shaped ones, a process that can be termed as electrospraying. Thus, electrospinning/electrospraying is a highly versatile technique for the fabrication of products, the shapes of which can be varied by control of the matrix concentration.[46,47]

Received: March 2, 2013
Accepted: June 10, 2013
Published: June 10, 2013

   dx.doi.org/10.1021/am400782s | ACS Appl. Mater. Interfaces 2013, 5, 6038−6044

Scheme 1. Schematic Diagram for Light-Emitting Electrospun Sheets Electrospun with (a) Single-Nozzle and (b and c) Multinozzle Equipment[a]

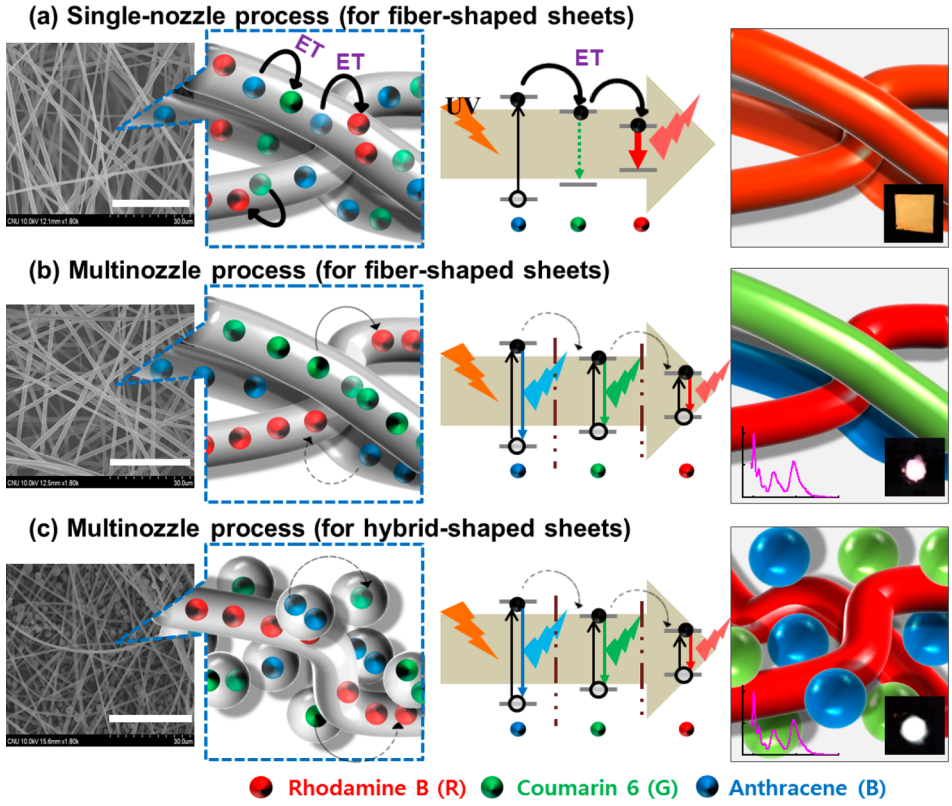

[a]ET between dyes can occur readily within fibers (S2F) electrospun with single-nozzle equipment because of the close proximity between dyes (a). ET can be efficiently blocked (M2F) using multinozzle equipment because of the nonaccessible distance between RGB dyes (b). (c) A hybrid-shaped sheet (M3H) composed of beads and fibers is also fabricated through a multinozzle electrospinning process. Inset photoraphs were taken of the emission of electrospun sheets coated on a commercial LED lamp (λ = 365 nm). The scale bar in FE-SEM images is 30 μm.

Flexible light-emitting devices (FLEDs) have received a great deal of attention as next-generation light sources because of their specific properties of flexibility, lightness, portability, and durability.[48−51] FLEDs can be fabricated by coating light-emitting materials onto flexible plastic substrates or films. However, because of the intrinsic disadvantages of conventional methods, such as the intricacy and expense involved in their production, electrospinning processes have gathered a lot of interest for the fabrication of FLEDs with lower associated cost as well as greater simplicity.

Herein, we suggest a simple fabrication method for emissive nanofibrous sheets composed of poly(methyl methacrylate) (PMMA) as a matrix polymer and RGB dyes as guest fluorophores at various ratios, which enable a facile color tuning for white emission via control of interactive ET between dyes, because of spatially isolated locations in electrospun products. Unlike the conventional use of complicated chemical functionalization of a polymer itself to prepare white-emitting materials, developed emissive sheets can be simply prepared by electrospinning with the polymer matrix (PMMA) in the presence of commercially available RGB dyes. The potentially separated RGB dyes in the polymer matrix electrospun with multinozzle equipment may allow for efficient control of ET between dyes. Thus, it becomes possible to tune the desirable emissive color by merely adjusting the concentration of each dye, which is used upon production. We demonstrated its application for white-light emission, using a commercial blue light-emitting-diode (LED) lamp as the excitation source.

EXPERIMENTAL SECTION

Materials. Poly(methyl methacrylate) (PMMA) was purchased from Sigma-Aldrich (MW = 120000). Red-, green-, and blue-emitting (RGB) dyes corresponding to rhodamine B, coumarin 6, and anthracene, respectively, were purchased from Sigma-Aldrich and used as received.

Electrospinning Process. PMMA solutions containing the appropriate dye concentrations based on PMMA for electrospinning were prepared in tetrahydrofuran (THF) and *N*,*N*-dimethylformamide (DMF) (1:1, v/v). In the case of fiber spinning, PMMA (30% w/v relative to the solvent) was dissolved in THF/DMF with suitable amounts of dyes. To fabricate bead-shaped products, more diluted PMMA solutions of 5% w/v were used. The dye-doped PMMA solutions were stirred at room temperature for over 8 h. The electrospinning apparatus consisted of a high-voltage power supply (Chungpa EMT Co., Ltd., CPS-40K03, Korea), a plate-shaped collector (NanoNC Co., ESR200R2, Korea), and a syringe pump with an airtight syringe needle (24 gauge) assembly. Electrospinning was performed at a potential of 6.5 kV, and the distance between the electrodes was maintained at 15 cm. The spinning rate was kept at 0.3 mL/h using a motorized syringe pump. Fiber- or bead-shaped sheets were deposited on aluminum foil on the collector as a ground electrode. All processes were carried out at ambient conditions, and the thickness of the electrospun sheets was controlled by adjusting the spinning time.

Characterization. A high-resolution field-emission scanning electron microscope (Jeol, JSM-700F) was used to collect electron micrographs of the electrospun fibers and beads. Fluorescence microscopic images of electrospun beads and fibers were taken using an Olympus BX53. Photoluminescence spectra were obtained using a

dx.doi.org/10.1021/am400782s | ACS Appl. Mater. Interfaces 2013, 5, 6038−6044

Cary Eclipse (Varian) fluorescence spectrometer equipped with a xenon lamp excitation source. The lifetimes of the electrospun sheets were measured with a time-resolved FL 900 fluorescence spectrometer equipped with a Mira model 900-P laser. Commercially avaiable blue LED lamp was used as an excitation source (λ = 365 nm, Seoul Optodevice Co., Ltd., T5F36, Korea), on which electrospun fibers are coated to obtain white illumination.

RESULTS AND DISCUSSION

The fluorescent PMMA solutions and resultant emissive electrospun sheets were prepared using three types of commercially available light-emitting dye molecules: rhodamine B (R), coumarin 6 (G), and anthracene (B) for red, green, and blue emissions, respectively. Absorption and fluorescence spectra of RGB dyes in chloroform solutions are illustrated in Figure S1 in the Supporting Information. The emission of B and the absorption of G and the emission of G and the absorption of R have good overlap, which means that ET between donor (B or G) and acceptor (G or R) dyes will occur if they are in close proximity. In turn, this will cause serious problems in tuning the emission properties of their mixed system.

Accordingly, only longest-wavelength emission (in this case, red) is expected if the RGB dyes are located altogether in a single fiber of PMMA host electrospun with single-nozzle equipment (Scheme 1a), because of spontaneous ET from blue to green and from green to red, even when excited at the absorption maximum of B. Thus, spatial isolation of each dye in separate fibers was conjectured using multinozzle equipment during an electrospinning process. Physical isolation of each dye should be achieved using separate incorporation of each RGB dye in each PMMA host followed by electrospinning of each PMMA solution, which is positioned at each nozzle in multinozzle electrospinning equipment. The amounts of dyes in PMMA fibers are optimized to obtain the desired emission spectra.

When the three different dyes are confined in the same fiber (from the single nozzle), the average donor-to-acceptor distance decreases below the Förster radius because of the dense packing within the fibers. That is, ET from blue to green and from green to red becomes remarkable within the fibers. In contrast, fibers or beads from multinozzle equipment containing the three different dyes in different fibers or beads provide separation of each dye to retard ET.

As a result, ET can be efficiently suppressed or retarded by spatially confined multicolored fiber or hybrid (fiber plus bead) systems, in which each dye is individually isolated in each fiber or fiber/bead, and consequently each RGB fluorescence can emit at different positions of the fibers or beads (Scheme 1b,c). The sample codes denote the nozzle used, dye feed ratios, and shape of the electrospun mats, such as M2F (multinozzle, ratio 2, and fiber-shaped), S4B (single nozzle, ratio 4, and bead-shaped), and M3H [multinozzle, ratio 3, and hybrid (fiber plus bead)-shaped].

We have fabricated RGB dye-doped PMMA electrospun sheets using multinozzle electrospinning (Scheme S1 in the Supporting Information). The multinozzle electrospinning equipment has a potential problem of electrical repulsion between the adjacent nozzles. To solve this problem, secondary electrodes are introduced next to syringes filled with red- and green-emitting solutions. A stable jet between the syringe needle assembly and the collector was obtained under these conditions. Therefore, electrospun fibers and beads from each nozzle are mixed homogeneously in the same location of the collector. Moreover, pitching and rolling of a plate-type collector in the system enables the fabrication of homogeneously emissive electrospun sheets.

The field-emission scanning electron microscopy (FE-SEM) images of various types of sheets including fiber-shaped, hybrid-shaped (fibers plus beads), and bead-shaped sheets, electrospun with the multinozzle equipment according to the concentrations of the matrix PMMA, are shown in Scheme 1. The average diameters of the fibers and beads were measured to be 2.2 and 2.1 μm, respectively, and are virtually uniform.

Figure 1 shows the emission spectra (excitation wavelength 365 nm) of light-emitting, electrospun sheets of PMMA

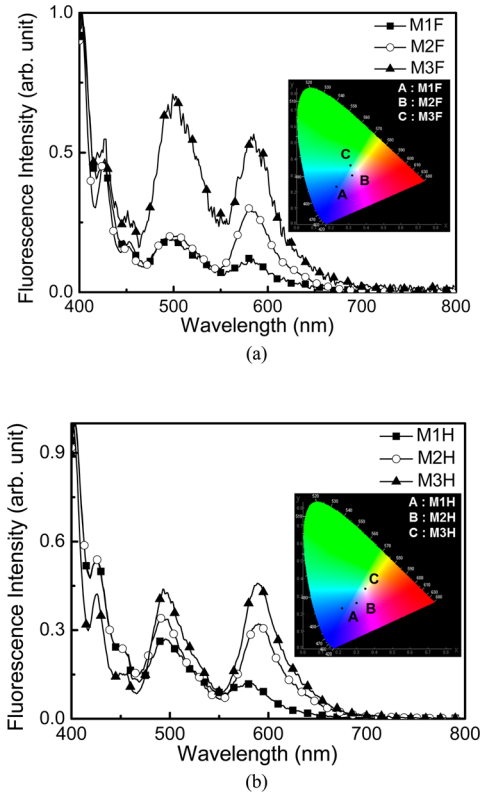

Figure 1. Changes in fluorescence spectra of light-emitting (a) fiber-shaped and (b) hybrid-shaped sheets upon increases in the concentrations of both R and G dyes (excitation wavelength λ_{ex} = 365 nm). The inset CIE diagrams show the chromaticity parameters approaching that of white color (0.33, 0.33).

matrixes with various concentration ratios of RGB dyes. Light-emitting sheets consisting of R, G, and B dyes in spatially separated fibers were fabricated (Figure 1a and Table 1). Fluorescence color can be easily tuned by a variation in the concentration of dyes, indicative of minimal ET. The clear and distinctive RGB bands in the fluorescence spectra of the separately incorporated dyes in the fibers indicate that each dye maintains its optical properties when incorporated into host PMMA fibers. This enables us to obtain close to white emission by measuring the Commission Internationale de 1′Eclairage (CIE) coordinates. Moreover, similar results (both color tuning and white emission) can be accomplished using even smaller amounts of dyes when hybrid (R in fibers; G and B in beads)-shaped sheets are constructed because smaller amounts of host PMMA are used for bead formation compared to that for fiber

dx.doi.org/10.1021/am400782s | ACS Appl. Mater. Interfaces 2013, 5, 6038−6044

Table 1. Variation of the CIE Coordinates of Light-Emitting PMMA Sheets by Changes in the Concentration Ratio of RGB Dyes[a]

method	shape	sample code[b]	R (wt %)	G (wt %)	B (wt %)	CIE index (x, y)
multinozzle	fiber	M1F	0.24 (0.0072 g)[c]	0.10 (0.003 g)[c]	3 (0.09 g)[c]	(0.23, 0.23)
multinozzle	fiber	M2F	0.25 (0.0075 g)[c]	0.14 (0.0042 g)[c]	3 (0.09 g)[c]	(0.32, 0.30)
multinozzle	fiber	M3F	0.31 (0.0093 g)[c]	0.22 (0.0066 g)[c]	3 (0.09 g)[c]	(0.31, 0.36)

[a]The PMMA concentration is 30% w/v in DMF/THF (1:1, v/v). The concentrations of the RGB dyes are based on the concentration of PMMA. [b]M denotes multinozzle, numbers denote the ratio, and F denotes fiber-shaped. [c]The numbers in parentheses correspond to absolute amounts of dyes in PMMA (3 g).

Table 2. Variation of the CIE Coordinates of Light-Emitting PMMA Sheets by Changes in the Concentration Ratio of RGB Dyes[a]

method	shape	sample code[b]	R (wt %)[c]	G (wt %)[d]	B (wt %)[d]	CIE index (x, y)
multinozzle	hybrid	M1H	0.25 (0.0075 g)[e]	0.5 (0.0025 g)[f]	3 (0.015 g)[f]	(0.22, 0.23)
multinozzle	hybrid	M2H	0.5 (0.015 g)[e]	0.5 (0.0025 g)[f]	3 (0.015 g)[f]	(0.30, 0.26)
multinozzle	hybrid	M3H	0.7 (0.021 g)[e]	0.7 (0.0035 g)[f]	3 (0.015 g)[f]	(0.35, 0.34)

[a]The concentration of PMMA for fiber formation is 30% w/v and that for bead formation is 5% w/v relative to the solvent [1:1 (v/v) DMF/THF]. The concentrations of the RGB dyes are based on the concentration of PMMA. [b]M denotes multinozzle, numbers denote the ratio, and H denotes hybrid (fiber plus bead)-shaped. [c]R is located in fibers. [d]G and B are located in beads. [e]The numbers in parentheses correspond to absolute amounts of dyes in PMMA (3 g) for fiber formation. [f]The numbers in parentheses correspond to absolute amounts of dyes in PMMA (0.5 g) for bead formation.

formation, as shown in Figure 1b and Table 2. According to the CIE coordinate values in Tables 1 and 2, the emission color can be successfully tuned using different ratios of RGB dyes. As shown in the two-dimensional projections of the CIE XY chromaticity diagrams (insets in Figure 1), M2F as fiber-shaped sheets with an RGB concentration ratio of 0.2:0.14:3 and M3H as hybrid-shaped sheets with an RGB concentration ratio of 0.7:0.7:3 show nearly pure white-light emission with CIE coordinates of (0.32, 0.30) and (0.35, 0.34), respectively, which is very close to the coordinate of the standard white-light illumination (0.33, 0.33). Because ET between donor and acceptor dyes is effectively retarded, the color spectrum can be tuned easily by varying the ratio between the three different emitting dyes.

However, emission color tuning becomes difficult if RGB dyes are located altogether within the same matrix (S2F, constructed with single-nozzle equipment) even using the same RGB ratios with M2F, irrespective of its shape, such as fiber or bead, as shown in Figure S2 and Table S1 in the Supporting Information. Considering the fact that the same ratios of RGB dyes in the sheets were used with the cases of M2F (same ratio with S2F) and M4B (same ratio with S4B), an increased intensity of the red emission of S2F and S4B (inset photographs in Figure S2 in the Supporting Information) can be observed mainly because of the facilitated ET. It can be concluded that fiber- and hybrid-shaped sheets electrospun with multinozzle equipment are able to maintain the spatially desirable separation between individual fluorophores, retarding unwanted ET and, as a result, enabling the construction of white-emitting sheets.

We obtained excitation profiles of the red dye in the single-nozzle and multinozzle electrospun fibers (Figure S3 in the Supporting Information). In the case of S2F, the excitation spectrum shows not only a peak of dye R but also peaks of B and G with high intensity. However, in the case of M2F, it shows B and G dyes with lower intensities than those of S2F. Although M2F and S2F contain the same amounts of RGB dyes, excitation spectra appeared differently, especially in wavelengths of B and G dyes. That means that the ET efficiencies of fiber-shaped sheets electrospun with multinozzle and single-nozzle equipment (M2F and S2F) are remarkably different.

Different from the all-fiber and hybrid systems constructed with multinozzle equipment, all-bead systems also have a disadvantage in tuning the emission color. This is presumably due to the scarce chance of ET resulting from the large separation between dyes (less contact area between spheres), leading to the need for more populations of red dye molecules. As shown in Figure S4 and Table S2 in the Supporting Information, the emission color was varied proportionally according to the RGB ratios, indicating the inadequacy of all-bead shapes for emission color tuning, even those electrospun with multinozzle equipment. The CIE coordinates exhibited difficulty in color tuning in both bead-shaped sheets produced through multinozzle electrospinning and other types of sheets produced through single-nozzle electrospinning (Figure S5 in the Supporting Information).

We prepared fiber-shaped sheets from single-nozzle equipment with a lower concentration of RGB dyes inside the fiber (S2F-1, S2F-2, and S2F-3). As concentrations of dyes inside the fiber decreased while maintaining an RGB dye ratio similar to that in S2F, fluorescence intensities of G and R dyes were considerably reduced (reduction is more noticeable in red) because of the increase in the distance between dyes inside the fiber, in which tuning the color for white emission (Figure S6 in the Supporting Information) is difficult.

We also tried to fabricate white-light-emitting sheets with single-nozzle equipment by decreasing the concentrations of G and R. Unfortunately, it was found that the intensities of G and R in electrospun sheets with single-nozzle equipment did not decrease proportionally by decreasing the concentrations of G and R, owing to the undesirable ET between dyes inside the fiber. Hence, S9F, in which the concentrations of G and R were one-tenth those in S2F, emits strong green light, not red light. Thus, to obtain white-light-emitting sheets, it is essentail to fabricate spatially separated fibers in matrixes with a controllable, partial ET between dyes by multinozzle electrospinning to attain easy and facile color tuning (Figure S7 in the Supporting Information).

Fluorescence microscopic analysis was carried out to verify the fact that individual RGB dyes fluoresce at different locations without interaction. Figure 2 shows fluorescence microscopic

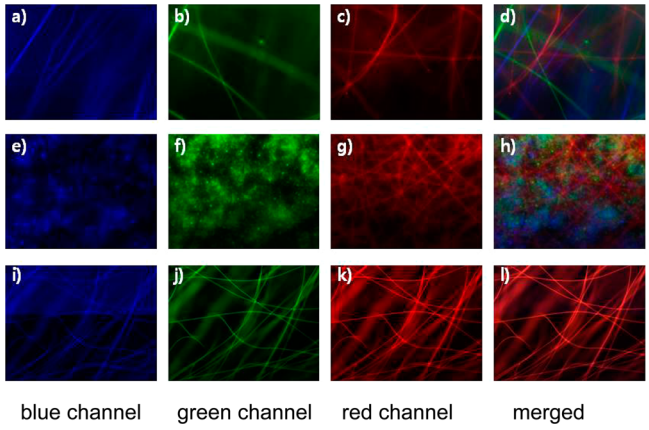

Figure 2. Fluorescence microscopic images of fiber-shaped M2F (a–d) with an RGB concentration ratio of 0.25:0.14:3 electrospun with multinozzle equipment, hybrid-shaped M3H (e–h) with an RGB concentration ratio of 0.7:0.7:3 electrospun with multinozzle equipment, and fiber-shaped S2F (i–l) with an RGB concentration ratio of 0.25:0.14:3 electrospun with single-nozzle equipment.

images of M2F, M3H, and S2F. As expected, distinctive, randomly distributed, spatially separated RGB emission colors in M2F and M3H sheets can be seen at different sites of fibers or beads with high spatial resolution (Figure 2a–c,e–g). Similarly, separate emission colors can also be seen from the fiber-shaped sheets (S2F) electrospun with single-nozzle equipment (Figure 2i–k). However, S2F emits three colors simultaneously from the same site of the fiber and, resultantly, emits red because of ET to red dye without spatial resolution (Figure 2l). The emission colors came from spatially separated, independent matrixes, which can be observed by a simple comparison of merged colors of the sheets electrospun with multinozzle equipment (Figure 2d, h) with those electrospun with single-nozzle equipment (Figure 2l).

To verify the retarded ET between dyes in the fiber- and bead-shaped sheets electrospun with multinozzle equipment quantitatively, the time-resolved fluorescence lifetimes of B and G dyes (at 410 and 500 nm, respectively), as donors, were investigated, as shown in Figure 3, and the data are tabulated in Table 3. When excited at 389 nm, the lifetimes of B at 410 nm and of G at 500 nm in M2F sheets are longer than those of B and G in S2F sheets (produced by single-nozzle equipment). This indicates that the donor dyes (B and G) located in separate fibers (M2F) have less chance to contact to the acceptor dye R, compared to the case of S2F sheets, of which RGB dyes are located within the same fiber, resulting in suppressed ET (Figure 3a). Similarly, B and G in bead-shaped sheets electrospun with multinozzle equipment (M4B) have longer lifetimes than those in bead-shaped sheets electrospun with single-nozzle equipment (S4B), in which both sheets have the same RGB ratio (Figure 3b). Therefore, it can be concluded that the positioning of RGB locations in separate fiber matrixes is the primary concern for the suppression of ET between dyes and to attain easy and facile color tuning.

To gain insight for the reduction of ET in spatially separated nanofibers by multinozzle electrospinning quantitatively, the ET efficiency was calculated based on the decay time of B dye

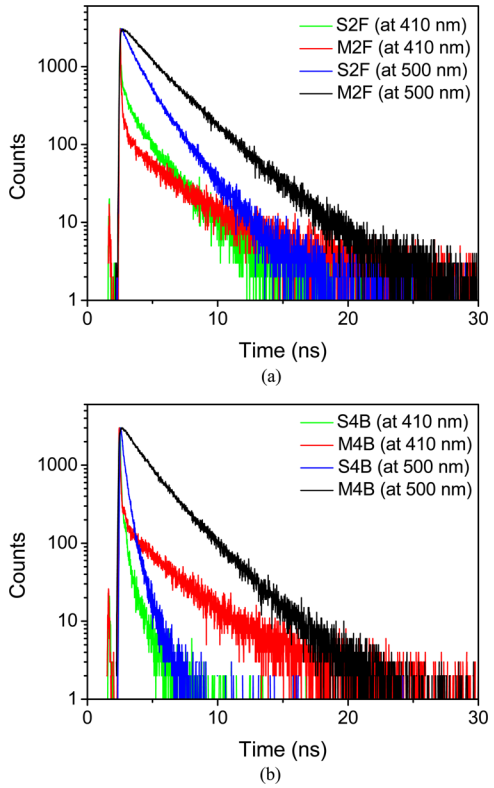

Figure 3. Time-resolved fluorescence decay profiles of (a) fiber-shaped and (b) bead-shaped sheets electrospun by single-nozzle (S2F and S4B) or multinozzle electrospinning equipment (M2F and M4B) at 410 and 500 nm upon excitation at 389 nm.

in fibers or in beads (Figure S8 in the Supporting Information). The ET efficiency was calculated by the equation $E = (1 - \tau_D'/\tau_D) \times 100$, where τ_D' and τ_D are the donor (B) fluorescence lifetimes in the presence and absence of the acceptor (G), respectively.[52] The ET efficiencies of fiber- and bead-shaped sheets electrospun by multinozzle equipment (M2F and M4B) and single-nozzle equipment (S2F and S4B) are tabulated in Table 3. The ET efficiencies for M2F and M4B are 12.7% and 2.8%, respectively. Meanwhile, the ET efficiencies for S2F and S4B were found to be 46.7% and 87.7%, respectively, which are much larger than the cases of M2F and M4B. This indicates that the ETs are much facilitated in the matrix electrospun by single-nozzle equipment, resulting from the close proximity of RGB dyes. As a result, control of ET can be accomplished with multinozzle equipment to obtain the expected color tuning.

To obtain a white-emitting sheet device, M2F and M3H are electrospun directly on the top of a commercially available blue LED lamp (λ = 365 nm; Figure S9 in the Supporting Information), which is used as an excitation light source. The inset photographs in Scheme 1b,c show the white-emitting sheets, which have been successfully constructed.

CONCLUSIONS

Emissive, electrospun sheets containing PMMA as a matrix polymer and RGB dyes provide a simple and easily obtainable method of the emission color tuning toward white-light emission upon excitation with a single source. The demonstration of white-light emission on a blue-emitting LED lamp as an excitation source also provides a new challenge for large-scale emissive materials. Such significant color tuning was possible because of the effective blocking of ET between dyes,

Table 3. Decay Times of Dyes (B at 410 nm and G at 500 nm) Located in Fiber- and Bead-Shaped Sheets Electrospun with Single-Nozzle and Multinozzle Equipments (Excitation at 389 nm)

			B at 410 nm		G at 500 nm		
shape	method	sample code[a]	τ_1 (%)/ns	τ_2 (%)/ns	τ_1 (%)/ns	τ_2 (%)/ns	efficiency (%)[b]
fiber	single nozzle	S2F	0.017 (53)	1.906 (47)	0.835 (43)	2.000 (57)	46.7
	multinozzle	M2F	0.028 (56)	3.329 (44)	1.484 (25)	2.910 (75)	12.7
bead	single nozzle	S4B	0.003 (69)	0.754 (31)	0.180 (68)	0.657 (32)	87.7
	multinozzle	M4B	0.004 (36)	2.917 (64)	1.185 (32)	2.571 (68)	2.8

[a]M and S denote multinozzle and single-nozzle equipment, respectively, numbers denote the ratio, and F and B denote fiber- and bead-shaped, respectively. [b]The ET efficiency was calculated by fluorescence lifetimes of the donor (dye B) in the presence and absence of the acceptor.

which allows facile color tuning by adjustment of the concentration of each dye. Compared to conventional chemical modification-based white-light-emitting systems, nanofibrous polymer sheets prepared by the electrospinning technique with multinozzle equipment could be exploited in flexible and large-scale applications.

■ ASSOCIATED CONTENT

Supporting Information

Absorption and emission spectra of RGB dyes, schematic diagrams for electrospinning equipment, and color tuning for other examples. This material is available free of charge via the Internet at http://pubs.acs.org.

■ AUTHOR INFORMATION

Corresponding Author

*E-mail: tslee@cnu.ac.kr. Phone: +82-42-821-6615. Website: http://www.onom.re.kr.

Notes

The authors declare no competing financial interest.

■ ACKNOWLEDGMENTS

Financial support from the National Research Foundation of Korea through Basic Science Research Program (2012R1A2A2A01004979) funded by the Korea government is gratefully acknowledged.

■ REFERENCES

(1) Nakajima, T.; Isobe, M.; Tshchiya, T.; Ueda, Y.; Kumagai, T. *Nat. Mater.* **2008**, *7*, 735−740.
(2) D'Andrade, B. W.; Forrest, S. R. *Adv. Mater.* **2004**, *16*, 1585−1595.
(3) Gather, M. C.; Köhnen, A.; Meerholz, K. *Adv. Mater.* **2011**, *23*, 233−248.
(4) Kwak, S.-Y.; Yang, S.; Kim, N. R.; Kim, J. H.; Bae, B.-S. *Adv. Mater.* **2011**, *23*, 5767−5772.
(5) Wang, F.; Chen, Y.; Liu, C.; Ma, D. *Chem. Commun.* **2011**, *47*, 3502−3504.
(6) Zhang, B.; Tan, G.; Lam, C.; Yao, B.; Ho, C.; Liu, L.; Xie, Z.; Wong, W.; Ding, J.; Wang, L. *Adv. Mater.* **2012**, *24*, 1873−1877.
(7) Zhang, L.; Hu, S.; Chen, J.; Chen, Z.; Wu, H.; Peng, J.; Cao, Y. *Adv. Funct. Mater.* **2011**, *21*, 3760−3769.
(8) Kamtekar, K. T.; Monkman, A. P.; Bryce, M. R. *Adv. Mater.* **2010**, *22*, 572−582.
(9) Krummacher, B. C.; Choong, V. E.; Mathai, M. K.; Choulis, S. A.; So, F.; Jermann, F.; Fiedler, T.; Zachau, M. *Appl. Phys. Lett.* **2006**, *88*, 113506.
(10) Liu, J.; Xie, Z.; Cheng, Y.; Geng, Y.; Wang, L.; Jing, X.; Wang, F. *Adv. Mater.* **2007**, *19*, 531−535.
(11) He, G.; Guo, D.; He, C.; Zhang, X.; Zhao, X.; Duan, C. *Angew. Chem., Int. Ed.* **2009**, *48*, 6132−6135.
(12) Bulovic, V.; Shoustikov, A.; Baldo, M. A.; Bose, E.; Kozlov, V. G.; Thompson, M. E.; Forrest, S. R. *Chem. Phys. Lett.* **1998**, *287*, 455−460.
(13) Tang, K.-C.; Chang, M.-J.; Lin, T.-Y.; Pan, H.-A.; Fang, T.-C.; Chen, K.-Y.; Hung, W.-Y.; Hsu, Y.-H.; Chou, P.-T. *J. Am. Chem. Soc.* **2011**, *133*, 17738−17745.
(14) Pimputkar, S.; Speck, J. S.; DenBaars, S. P.; Nakamura, S. *Nat. Photonics* **2009**, *3*, 179−181.
(15) Gong, X.; Wang, S.; Moses, D.; Bazan, G. C.; Heeger, A. J. *Adv. Mater.* **2005**, *17*, 2053−2058.
(16) Kim, J.-H.; Kim, K.-S.; Yoo, S. I.; Sohn, B.-H. *Thin Solid Films* **2011**, *519*, 8161−8165.
(17) Kim, K.-S.; Yoo, S. I.; Kim, M.; Sohn, B.-H. *Macromol. Chem. Phys.* **2010**, *211*, 2382−2388.
(18) Hendler, N.; Belgorodsky, B.; Mentovich, E. D.; Gozin, M.; Richter, S. *Adv. Mater.* **2011**, *23*, 4261−4264.
(19) Ma, J. C.; Dougherty, D. A. *Chem. Rev.* **1997**, *97*, 1303−1324.
(20) Mckay, S. L.; Haptonstall, B.; Gellman, S. H. *J. Am. Chem. Soc.* **2011**, *123*, 1244−1245.
(21) Dzenis, Y. *Science* **2004**, *304*, 1917−1919.
(22) Fong, H. In *Polymeric Nanostructures and Their Applications*; Nalwa, H. S., Ed.; American Scientific Publishers: Stevenson Ranch, CA, 2007; Vol. *2*, pp 451−474.
(23) Greiner, A.; Wendorff, J. H. *Angew. Chem., Int. Ed.* **2007**, *46*, 5670−5703.
(24) Luo, C. J.; Stoyanov, S. D.; Stride, E.; Pelan, E.; Edirisinghe, M. *Chem. Soc. Rev.* **2012**, *41*, 4708−4735.
(25) Li, D.; Xia, Y. *Adv. Mater.* **2004**, *16*, 1151−1170.
(26) Reneker, D. H.; Yarin, A. L.; Zussman, E.; Xu, H. *Adv. Appl. Mech.* **2007**, *41*, 43−195.
(27) Greiner, A.; Wendorff, J. H. *Adv. Polym. Sci.* **2008**, *219*, 107−171.
(28) Agarwal, S.; Wendorff, J. H.; Greiner, A. *Polymer* **2008**, *49*, 5603−5718.
(29) Li, D.; Xiao, Y. *Nano Lett.* **2004**, *4*, 933−938.
(30) Madhugiri, S.; Dalton, A.; Gutierrez, J.; Ferraris, J. P.; Balkus, K. J. *J. Am. Chem. Soc.* **2003**, *125*, 14531−14538.
(31) Babel, A.; Li, D.; Xia, Y. N.; Jenekhe, S. A. *Macromolecules* **2005**, *38*, 4705−4711.
(32) Dong, H.; Fey, E.; Gandelman, A.; Jones, W. E. *Chem. Mater.* **2006**, *18*, 2008−2011.
(33) Bashouti, M.; Salalha, W.; Brumer, M.; Zussman, E.; Lifshitz, E. *ChemPhysChem* **2006**, *7*, 102−106.
(34) Bianco, A.; Bertarelli, C.; Frisk, S.; Rabolt, J. F.; Gallazzi, M. C.; Zerbi, G. *Synth. Met.* **2007**, *157*, 276−281.
(35) He, D.; Hu, B.; Yao, Q.-F.; Wang, K.; Yu, S.-H. *ACS Nano* **2009**, *3*, 3993−4002.
(36) Farrar, D.; Ren, K.; Cheng, D.; Kim, S.; Moon, W.; Wilson, W. L.; West, J. E.; Yu, S. M. *Adv. Mater.* **2011**, *23*, 3954−3958.
(37) Moran-Mirabal, J. M.; Slinker, J. D.; DeFranco, J. A; Verbridge, S. S.; Ilic, R.; Flores-Torres, S.; Abruna, H.; Malliaras, G. G.; Craighead, H. G. *Nano Lett.* **2007**, *7*, 458−63.
(38) Davix, B. W.; Niamnont, N.; Hare, C. D.; Sukwattanasinitt, M.; Cheng, Q. *ACS Appl. Mater. Interfaces* **2010**, *2*, 1798−1803.
(39) Yoon, J.; Chae, S. K.; Kim, J.-M. *J. Am. Chem. Soc.* **2007**, *129*, 3038−3039.

(40) Vohra, V.; Giovanella, U.; Tubino, R.; Murata, H.; Botta, C. *ACS Nano* **2011**, *5*, 5572−5578.
(41) Niu, Q.; Zhou, Y.; Wang, L.; Peng, J.; Wang, J.; Pei, J.; Cao, Y. *Adv. Mater.* **2008**, *20*, 964−969.
(42) Wang, X. Y.; Drew, C.; Lee, S. H.; Senecal, K. J.; Kumar, J.; Samuelson, L. A. *Nano Lett.* **2002**, *2*, 1273−1275.
(43) Long, Y. Y.; Chen, H. B.; Yang, Y.; Wang, H. M.; Yang, Y. F.; Li, N.; Li, K. A.; Pei, J.; Liu, F. *Macromolecules* **2009**, *42*, 6501−6509.
(44) Tao, S. Y.; Li, G. T.; Yin, J. X. *J. Mater. Chem.* **2007**, *17*, 2730−2736.
(45) Wang, Y.; La, A.; Ding, Y.; Liu, Y.; Lei, Y. *Adv. Funct. Mater.* **2012**, *22*, 3547−3555.
(46) George, M. C.; Braun, P. V. *Angew. Chem., Int. Ed.* **2009**, *48*, 8606−8609.
(47) Meziani, M. J.; Pathak, P.; Hurezeanu, R.; Thies, M. C.; Enick, R. M.; Sun, Y.-P. *Angew. Chem., Int. Ed.* **2004**, *43*, 704−707.
(48) Bae, S.; Kim, H.; Lee, Y.; Xu, X.; Park, J.; Zheng, Y.; Balakrishnan, J.; Lei, T.; Kim, H. R.; Song, Y. I.; Kim, Y.; Kim, K. S.; Ozyilmz, B.; Ahn, J.; Hong, B. H; Iijima, S. *Nat. Nanotechnol.* **2010**, *5*, 574−578.
(49) Ju, S.; Li, J.; Liu, J.; Chen, P.; Ha, Y.; Ishikawa, F.; Chang, H.; Zhou, C.; Facchetti, A.; Janes, D. B.; Marks, T. J. *Nano Lett.* **2008**, *8*, 997−1004.
(50) Chen, A.; Au, J.; Kazlas, A.; Gates, R. H.; McCreary, M. *Nature* **2003**, *423*, 136.
(51) Kim, S.; Kwon, H.-J.; Lee, S.; Shim, H.; Chun, Y.; Choi, W.; Kwack, J.; Han, D.; Song, M.; Kim, S.; Mohammadi, S.; Kee, I.; Lee, S. Y. *Adv. Mater.* **2011**, *23*, 3511−3516.
(52) Majoul, I.; Jia, Y.; Duden, R. In *Handbook of Biological Confocal Microscopy*, 3rd ed.; Pawley, J. B., Ed.; Springer: New York, 2006; pp 788−808.